Simulating an extreme over-the-horizon optical propagation event over Lake Michigan using a coupled mesoscale modeling and ray tracing framework

Basu, Sukanta

DOI
10.1117/1.OE.56.7.071505

Publication date
2017

Document Version
Final published version

Published in
Optical Engineering

Optical Engineering

OpticalEngineering.SPIEDigitalLibrary.org

Simulating an extreme over-the-horizon optical propagation event over Lake Michigan using a coupled mesoscale modeling and ray tracing framework

Sukanta Basu

SPIE.

Sukanta Basu, "Simulating an extreme over-the-horizon optical propagation event over Lake Michigan using a coupled mesoscale modeling and ray tracing framework," *Opt. Eng.* **56**(7), 071505 (2017), doi: 10.1117/1.OE.56.7.071505.

Simulating an extreme over-the-horizon optical propagation event over Lake Michigan using a coupled mesoscale modeling and ray tracing framework

Sukanta Basu*
Delft University of Technology, Faculty of Civil Engineering and Geosciences, Delft, The Netherlands

Abstract. Accurate simulation and forecasting of over-the-horizon propagation events are essential for various civilian and defense applications. We demonstrate the prowess of a newly proposed coupled mesoscale modeling and ray tracing framework in reproducing such an event. Wherever possible, routinely measured meteorological data from various platforms (e.g., radar and satellite) are utilized to corroborate the simulated results. [DOI: 10.1117/1.OE.56.7.071505]

Keywords: aerosol; mesoscale; refraction; stratification.

Paper 161804SS received Nov. 17, 2016; accepted for publication Feb. 2, 2017; published online Feb. 21, 2017.

1 Introduction

Owing to the curvature of the earth, the horizon-limited range (HLR) is rather limited. For an observer height of h_o and a target height of h_T, the HLR can be approximated as[1]

$$\mathrm{HLR} = \sqrt{2R_E}\left(\sqrt{h_o} + \sqrt{h_T}\right), \tag{1}$$

where R_E is the Earth's radius (= 6366200 m). Thus, in the absence of an atmosphere (i.e., vacuum condition), a typical skyscraper of height $h_T = 100$ m would only be visible up to a range of ~40 km.

Nonetheless, over the years, a number of unusual sightings of urban skylines well beyond the HLR have been documented by popular media around the world. One such over-the-horizon (OTH) image formation event was reported by the local press at Grand Haven, Michigan, on the night of May 10 to 11, 2012. It was claimed that, on that night, the lights from the skyline of Milwaukee, Wisconsin, were clearly visible from the shoreline of Lake Michigan at Grand Haven [see Fig. 1(a)]. Since the distance between Grand Haven and Milwaukee is ~125 km (≫HLR), it is reasonable to deduce that unusual atmospheric effects were at the root of this event. In this paper, utilizing a newly proposed coupled mesoscale modeling and ray tracing (henceforth CMMRT) framework[5,6] in conjunction with routine meteorological observations, we attempt to "shed some light" on this anomalous propagation event.

2 Analysis of Observational Data

According to the synoptic meteorological map [Fig. 1(b)], a strong high-pressure system was located on top of Lake Michigan around 0 coordinated universal time (UTC), May 11, 2012. This type of meteorological setting is commonly associated with a clear sky condition along with near-surface temperature stratification (also known as inversion). Since an inversion condition is a prerequisite for super-refractive effects [the vertical gradient of refractive index is negative during super-refractive conditions. As a result, in the case of (near) horizontal propagation, optical rays bend downward (toward the Earth's surface) instead of traveling in straight-line trajectories. Under such atmospheric conditions, target detection beyond the HLR is often feasible[1]], it is physically plausible that such an optical environment prevailed over Lake Michigan on this particular night.

Indeed, the signature of super-refraction is evident in the meteorological radar echoes. Throughout the night, a number of radar echoes propagated across Lake Michigan. An illustrative example is shown in Fig. 1(c). It is clear that the littoral boundary layer was quite conducive to RF wave propagation. However, given the significant disparity between RF and optical wavelengths,[7] this radar image does not provide any quantitative information about optical wave propagation. In fact, rigorous optical ray tracing calculations are needed for an in-depth characterization. Such results are reported in Sec. 4.

One of the most common (and reliable) variables for quantifying the near-surface refractive condition is the air–sea temperature difference (ASTD).[8,9] Positive (negative) values of ASTD are associated with super-refractive (subrefractive) conditions. Unfortunately, due to the low density of meteorological stations on Lake Michigan and along its shorelines, an accurate estimation of the ASTD values is not feasible for the propagation path between Grand Haven and Milwaukee. Under similar data-sparse situations, the atmospheric optics community commonly invokes the assumption of horizontal homogeneity.[8–12] The shortcomings of such an unphysical assumption were clearly illustrated by van Eijk and Kunz.[13] In this study, we make use of satellite-based data in tandem with *in-situ* measurements to avoid the assumption of homogeneity.

In Fig. 1(d), a satellite-based lake water temperature map is shown. Using a diverse suite of satellite observations (e.g., NASA's AMSRE and MODIS products), the NASA Jet Propulsion Laboratory (JPL) produced this optimally

*Address all correspondence to: Sukanta Basu, E-mail: s.basu@tudelft.nl

0091-3286/2017/$25.00 © 2017 SPIE

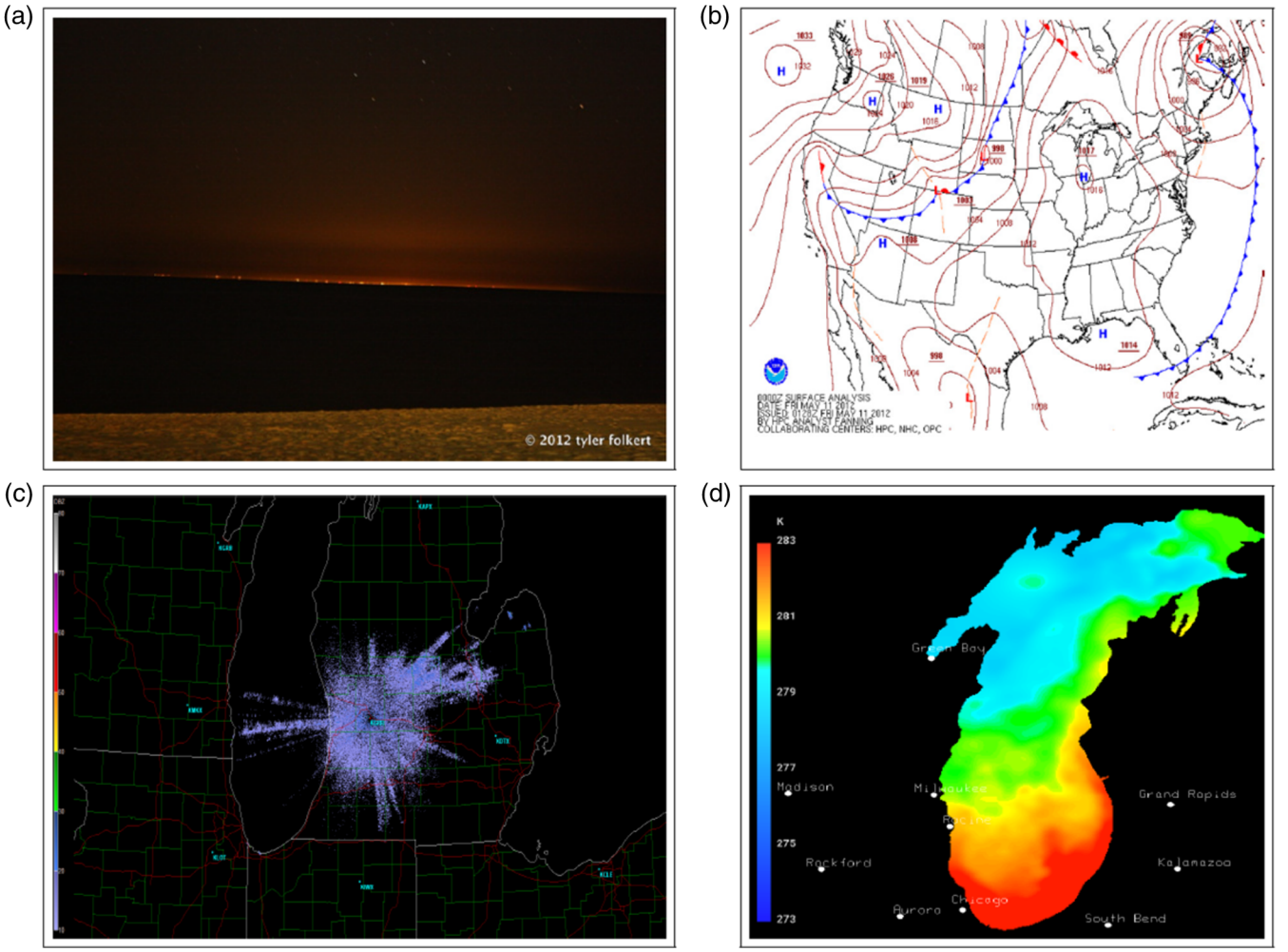

Fig. 1 (a) View of Milwaukee skyline from Grand Haven on the night of May 10 to 11, 2012 (Image courtesy: Tyler Folkert), (b) synoptic map of contiguous United States at 0 UTC, May 11, 2012 (source: Ref. 2), and (c) a reflectivity image from an NEXRAD radar at Grand Rapids (near Grand Haven). This image corresponds to 06:22 UTC. Signatures of super-refraction over Lake Michigan are clearly evident in these radar echoes. The radar data were downloaded from Ref. 3. (d) Satellite-based skin temperature map of Lake Michigan on May 11, 2012 (data source: NASA JPL[4]).

merged temperature dataset (known as the GHRSST dataset). Since the lake water temperature field has a very slow dynamical time-scale (due to the high specific heat capacity of water), we assume that this map is valid for the entire night.

Although satellite-derived sea surface (including lake water) temperature data are widely used by the scientific community, reliable measurement of near-surface air temperature via remote sensing is still a technical challenge. In this case, *in-situ* measurements from meteorological stations are our only viable option. Near our region of interest, four such stations (named MKGM4, HLNM4, 45007, and MLWW3) continuously measure near-surface air temperature data. However, water temperature measurements are only available from station 45007. The locations of all these stations are demarcated in a latter plot. Time-series observations of both air and water temperatures are shown in Fig. 2(a). Clearly, the air temperature measurements portray strong dependency on locations. Spatial heterogeneity was also evident in the satellite-based lake water temperature map of Fig. 1. As a consequence, the estimated ASTD values also show pronounced spatial variability. Based on the *in-situ* and satellite data, the observed ASTD value at the station MLWW3 (in close proximity to Milwaukee) was found to be remarkably high (on the order of 5 K), and it remained relatively constant over time. In other words, strongly stratified conditions persisted here throughout the night. In contrast, the ASTD values near Grand Haven (i.e., stations MKGM4 and HLNM4) represented weakly stratified (almost neutral) conditions. In Sec. 4, we will report similar findings based on numerical modeling.

Last, we would like to point out that, during that night, the winds were relatively calm over Lake Michigan. For all the stations, the surface wind speeds barely crossed 5 $\mathrm{m\,s^{-1}}$ [refer to Fig. 2(b)]. As a result, stratified layers were not destroyed (i.e., vertically mixed) by shear-generated turbulence.

Thus far, we have partially reconstructed the environmental setting for the night of May 10 to 11 utilizing a limited amount of routinely measured observational data. Undoubtedly, we have gained valuable insight through this analysis. However, we need more extensive data coverage (spanning well beyond

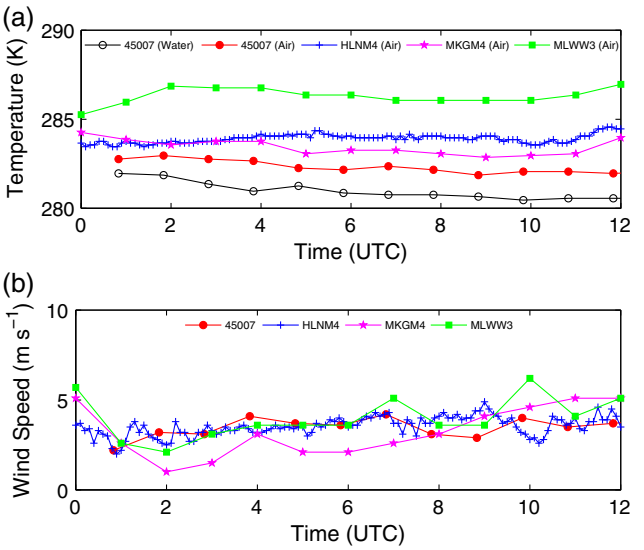

Fig. 2 Observed time-series of (a) air and water temperature and (b) wind speed from four meteorological stations. The air temperature sensors were located at the heights of 4 m (station 45007), 6.1 m (station MKGM4), 6.3 m (station HLNM4), and 9.1 m (station MLWW3) from the surface. The anemometers were located at the heights of 5 m (station 45007), 24.4 m (station MKGM4), 10.4 m (station HLNM4), and 12.2 m (station MLWW3), respectively. Data source: National Data Buoy Center.[14]

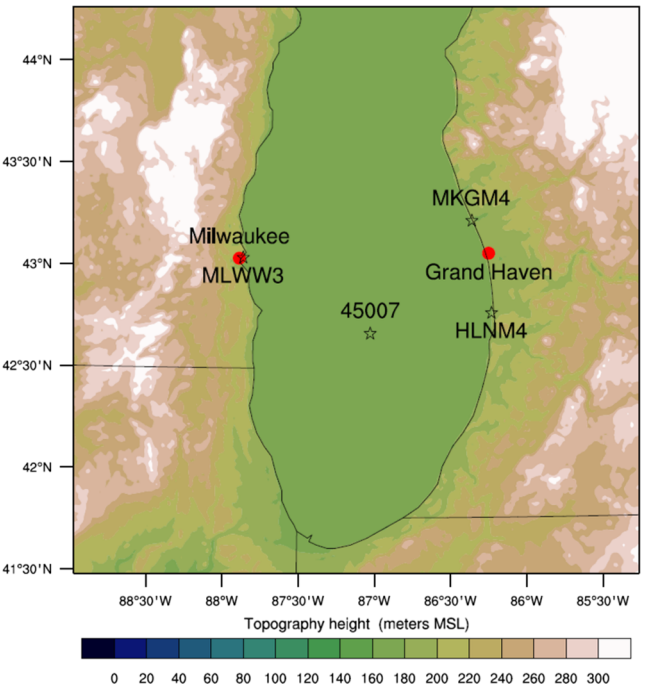

Fig. 3 The inner domain (d02) for the WRF simulation. The underlying topographic data are taken from the USGS. The locations of Grand Haven and Milwaukee are marked with filled red circles. The meteorological stations (MKGM4, HLNM4, 45007, and MLWW3) are depicted by black stars.

the near-surface region) to provide stronger evidence supporting the formation of an OTH image. We demonstrate that our newly proposed CMMRT framework[5,6] has the ability to accomplish such a challenging task.

3 Modeling Approach

In our CMMRT framework,[5,6] we couple a state-of-the-art atmospheric model, called the Weather Research and Forecasting (WRF) model,[15] with a ray tracing code to quantify the effects of atmospheric conditions on optical wave propagation. The WRF model is a nonhydrostatic mesoscale model that is capable of simulating a plethora of atmospheric phenomena ranging from hurricanes[16] to low-level jets[17] and from von Kármán vortex streets[18] to tornado outbreaks.[19]

3.1 *Mesoscale Modeling*

In this study, version 3.6.1 of the WRF model is employed to reconstruct the meteorological conditions around the time of the OTH propagation event. The following physics parameterizations are utilized: (i) planetary boundary layer: Yonsei University (YSU) scheme,[20,21] (ii) surface layer: Monin–Obukhov similarity-based scheme,[22] (iii) land surface: Noah scheme,[23] (iv) shortwave and longwave radiation: rapid radiative transfer model for global climate models (RRTMG) scheme,[24,25] and (v) microphysics: WRF single-moment 5-class scheme.[26] Most of these parameterization schemes are discussed in great detail by Stensrud.[27]

Two nested domains with one-way coupling are used in the simulation. The outer domain (d01) employs a horizontal grid resolution of 3 km × 3 km, whereas the inner domain (d02) uses a grid resolution of 1 km × 1 km (refer to Fig. 3). In both domains, 51 nonuniformly stretched vertical levels are used. The lowest model level is at ~8 m above ground level (AGL); the top of the domain is close to 16,000 m AGL. Approximately 18 vertical levels are below 1 km AGL. Land use and topographical properties for the simulation are taken from the United States Geological Survey (USGS) dataset at resolutions comparable with the horizontal grid resolution.

Similar to all computational fluid dynamics models, the WRF model requires initial and boundary condition data to initiate and time integrate atmospheric simulations. For the case study presented here, the WRF model is prescribed with meteorological initialization conditions from the North American Model (NAM; grid identifier 218; resolution: 12 km) analysis dataset. The WRF simulation is run for a total of 24 h with the first 12 h being used as spin-up time. The simulation start time is 12 UTC on May 10, 2012. The integration time-steps are 15 and 5 s for the d01 and d02 domains, respectively.

3.2 *Optical Ray Tracing*

Our ray tracing code has been described in details by Nunalee et al.[5] and He et al.[6] and will not be elaborated here. Briefly, the salient features of our modeling approach are as follows:

- Four-dimensional (4-D) temperature, moisture, and pressure fields from the WRF model-generated output are utilized as input.
- Ciddor's formulation[28] is invoked to compute the 4-D field of refractivity based on simulated temperature, moisture, and pressure fields.
- The ray tracing calculations are performed on a two-dimensional plane given by the line from observer to target and the center of the Earth. Realistic

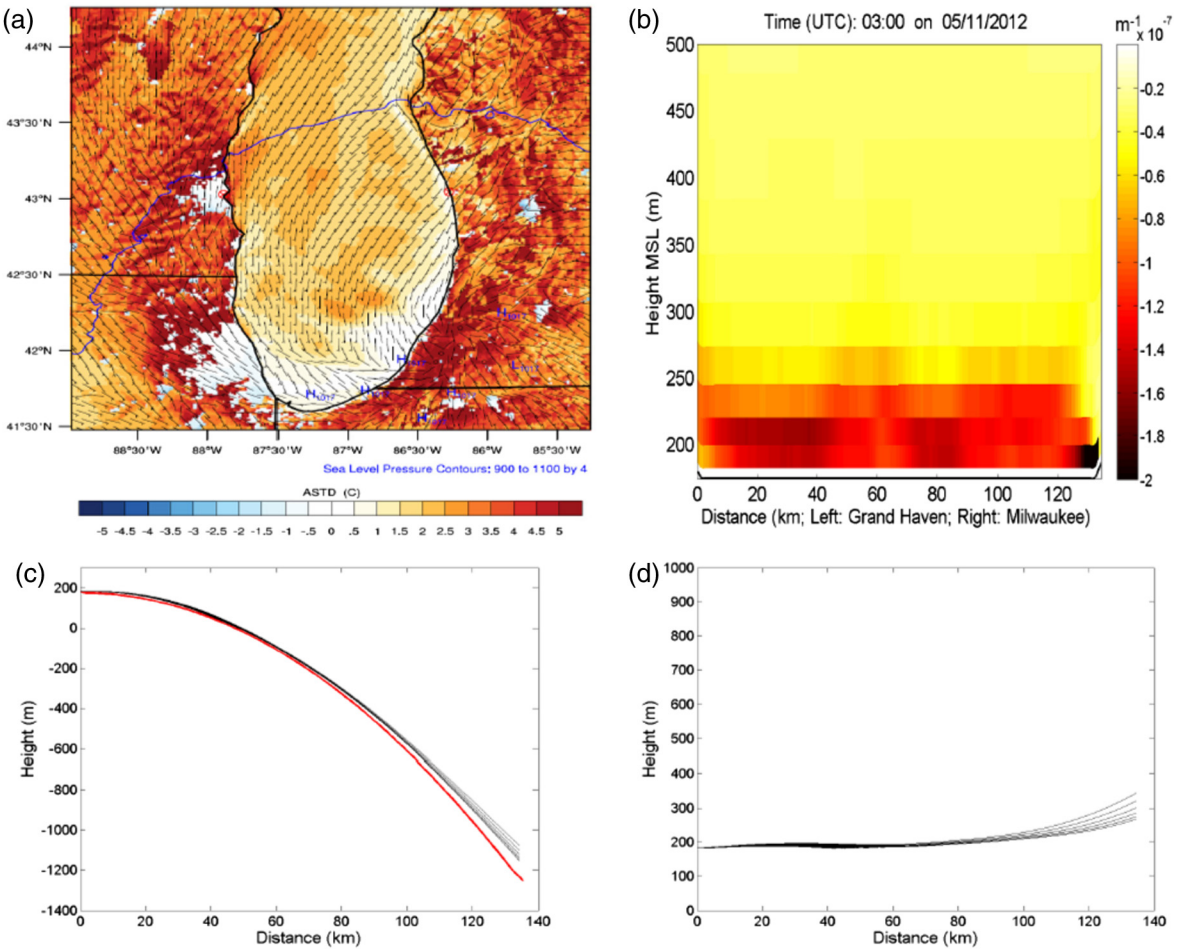

Fig. 4 (a) The WRF model-generated ASTD field at 3 UTC, May 11, 2012, (b) cross section of simulated refractive index gradient field between Grand Haven and Milwaukee, and (c) ray tracing along the cross section shown in (b). The height of the ray origin is at 2 m from the ground. Only the rays corresponding to elevation angles of 0 to 0.4×10^{-3} radians are shown. The red line portrays the earth's curvature. The ray trajectories in the flat-earth co-ordinate system[11] are shown in (d). Please note that the heights in the bottom figures use the mean sea level as datum.

topography from the WRF model is overlaid on a parabolic Earth model by Lehn.[29]

- The Eikonal equations are solved following a numerical approach proposed by Southwell.[30] A relatively fine spatial discretization size of 50 m is chosen for all ray tracing calculations to ensure numerical accuracy.[31]

4 Simulated Results

The simulated ASTD map is shown in Fig. 4(a). The results are in complete agreement with our earlier observational analysis. Clearly, the near-surface stratification is much stronger near Milwaukee in comparison to Grand Haven. Similar inferences can be made using Fig. 4(b). Furthermore, according to this simulated time-height plot, the refractivity gradients were quite strong within the lowest ~100 m of the littoral boundary layer (not just near the surface). This finding is very relevant for long-range propagation where optical rays tend to interact with elevated refractive layers.

Utilizing the simulated refractivity field as input, we perform ray tracing between Grand Haven (origin) and Milwaukee (target). A total of one thousand rays (wave length = 532 nm) uniformly distributed between −0.01 and +0.01 radians are released. The origin of the rays is taken at a height of 2 m from the ground. The results are shown in the bottom panels of Fig. 4. For low elevation angles (0 to 0.4 mrad), the rays closely follow the curvature of the Earth. The maximum deviation near Milwaukee is about 150 m. According to Wikipedia, the tallest skyscraper in Milwaukee is 183 m tall. In addition, there are eight other buildings that are taller than 100 m. Thus, based on our numerical simulations supported by observational analysis, lights from these buildings surely would have reached Grand Haven on the nights of May 10 to 11, 2012. Therefore, the claims made by the local media at Grand Haven are indeed credible and cannot be refuted.

5 Concluding Remarks

Extending the visibility range beyond the HLR is highly desirable for various applications including (but not limited to) active imaging, long-range video surveillance, laser target tracking, and electro-optical communications.[32–34] Such OTH viewing is feasible under certain meteorological conditions. In this paper, we focused on one such setting: super-refraction. Scattering and diffusion from aerosols can also lead to OTH image formation.[32] Since the existing

CMMRT framework is not capable of simulating aerosols in a realistic manner, we will utilize the WRF-CHEM model[35] in our future work. This upcoming framework will not only account for coherent mesoscale motions and turbulence but will also allow reliable calculation of aerosols, aerosol distribution morphology, and gas-phase chemistry (e.g., nucleation).

Acknowledgments

The author acknowledges financial support received from the US Department of Defense (AFOSR Grant under Award No. FA9550-12-1-0449). Any opinions, findings, and conclusions or recommendations expressed in this material are those of the author and do not necessarily reflect the views of the US Department of Defense.

References

1. D. Dion, "Refraction effects on EO system detection ranges in coastal environments," in *AGARD Conf. Proc. 576, Propagation Assessment in Coastal Environments* (1995).
2. www.wpc.ncep.noaa.gov.
3. www.ncdc.noaa.gov.
4. http://podaac.jpl.nasa.gov.
5. C. G. Nunalee et al., "Mapping optical ray trajectories through island wake vortices," *Meteorol. Atmos. Phys.* **127**, 355–368 (2015).
6. P. He et al., "Influence of heterogeneous refractivity on optical wave propagation in coastal environments," *Meteorol. Atmos. Phys.* **127**, 685–699 (2015).
7. E. E. Gossard et al., "The fine structure of elevated refractive layers: implications for over-the-horizon propagation and radar sounding systems," *Radio Sci.* **19**, 1523–1533 (1984).
8. K. Stein, E. Polnau, and D. Seiffer, "IR propagation through the marine boundary layer—comparison of model and experimental data," *Proc. SPIE* **4884**, 84–94 (2003).
9. D. Dion et al., "Raypath deviation under stable and unstable conditions," *Proc. SPIE* **5981**, 598109 (2005).
10. D. Dion et al., "Calculation and simulation of atmospheric refraction effects in maritime environments," *Proc. SPIE* **4167**, 1–9 (2001).
11. S. M. Doss-Hammel et al., "Low-altitude infrared propagation in a coastal zone: refraction and scattering," *Appl. Opt.* **41**, 3706–3724 (2002).
12. G. J. Kunz et al., "EOSTAR: an electro-optical sensor performance model for predicting atmospheric refraction, turbulence, and transmission in the marine surface layer," *Proc. SPIE* **5237**, 81–92 (2004).
13. A. M. J. van Eijk and G. J. Kunz, "The introduction of horizontal inhomogeneity of meteorological conditions in the EOSTAR propagation model," *Proc. SPIE* **6303**, 1–8 (2006).
14. http://www.ndbc.noaa.gov/.
15. W. C. Skamarock et al., "A description of the Advanced Research WRF version 3," Tech. Rep. NCAR/TN-475+STR, National Center for Atmospheric Research (2008).
16. C. Davis et al., "Prediction of landfalling hurricanes with the advanced hurricane WRF model," *Mon. Weather Rev.* **136**, 1990–2005 (2008).
17. B. Storm et al., "Evaluation of the Weather Research and Forecasting model on forecasting low-level jets: implications for wind energy," *Wind Energy* **12**, 81–90 (2009).
18. C. G. Nunalee and S. Basu, "On the periodicity of atmospheric von Kármán vortex streets," *Environ. Fluid Mech.* **14**, 1335–1355 (2013).
19. C. M. Shafer et al., "Evaluation of WRF forecasts of tornadic and nontornadic outbreaks when initialized with synoptic-scale input," *Mon. Weather Rev.* **137**, 1250–1271 (2009).
20. S.-Y. Hong, Y. Noh, and J. Dudhia, "A new vertical diffusion package with an explicit treatment of entrainment processes," *Mon. Weather Rev.* **134**(9), 2318–2341 (2006).
21. S.-Y. Hong, "A new stable boundary-layer mixing scheme and its impact on the simulated East Asian summer monsoon," *Q. J. R. Meteorol. Soc.* **136**, 1481–1496 (2010).
22. P. A. Jiménez et al., "A revised scheme for the WRF surface layer formulation," *Mon. Weather Rev.* **140**, 898–918 (2012).
23. F. Chen and J. Dudhia, "Coupling an advanced land surface-hydrology model with the Penn State-NCAR MM5 modeling system. Part I: Model implementation and sensitivity," *Mon. Weather Rev.* **129**, 569–585 (2001).
24. M. J. Iacono et al., "Radiative forcing by long-lived greenhouse gases: calculations with the AER radiative transfer models," *J. Geophys. Res.* **113**, 1–8 (2008).
25. E. J. Mlawer et al., "Radiative transfer for inhomogeneous atmospheres: RRTM, a validated correlated-k model for the longwave," *J. Geophys. Res.* **102**, 16663–16682 (1997).
26. S.-Y. Hong, J. Dudhia, and S.-H. Chen, "A revised approach to ice microphysical processes for the bulk parameterization of clouds and precipitation," *Mon. Weather Rev.* **132**, 103–120 (2004).
27. D. J. Stensrud, *Parameterization Schemes: Keys to Understanding Numerical Weather Prediction Models*, Cambridge University Press, Cambridge, UK, p. 459 (2007).
28. P. E. Ciddor, "Refractive index of air: new equations for the visible and near infrared," *Appl. Opt.* **35**, 1566–1573 (1996).
29. W. H. Lehn, "A simple parabolic model for the optics of the atmospheric surface layer," *Appl. Math. Model.* **9**, 447–453 (1985).
30. W. H. Southwell, "Ray tracing in gradient-index media," *J. Opt. Soc. Am.* **72**, 908–911 (1982).
31. J. Puchalski, "Numerical determination of ray tracing: a new method," *Appl. Opt.* **31**, 6789–6799 (1992).
32. G. C. Mooradian et al., "Over-the-horizon optical propagation in a maritime environment," *Appl. Opt.* **19**, 11–30 (1980).
33. M. T. Smith and M. C. Roggemann, "Pseudo-guide wave propagation in stratified, inverted temperature distributions in the atmosphere," in *2014 IEEE Aerospace Conf.*, pp. 1–7 (2014).
34. V. V. Belov et al., "Over-the-horizon optoelectronic communication systems," *Russian Phys. J.* **57**, 963–968 (2014).
35. G. A. Grell et al., "Fully coupled "online" chemistry within the WRF model," *Atmos. Environ.* **39**, 6957–6975 (2005).

Sukanta Basu is an associate professor at Delft University of Technology. He received his PhD in civil engineering from the University of Minnesota in 2004. His current research interests include atmospheric optics, turbulence modeling, and numerical weather prediction. His research has been disseminated through more than 40 peer-reviewed publications in the fields of fluid mechanics, meteorology, nonlinear physics, atmospheric optics, and engineering. He is a member of SPIE.